Desalination and Water Treatment
www.deswater.com

doi:10.5004/dwt.2019.24633

166 (2019) 122–134
October

Optimization and mechanism pathways of *p*-cresol decomposition over Cu-Fe/NaP1 catalyst by Fenton-like process

Kitirote Wantala[a,b,c,d,*], Wasipim Chansiriwat[a,b], Rattabal Khunphonoi[b,d,e], Chatkamol Kaewbuddee[a,b], Totsaporn Suwannaruang[a,b], Narong Chanlek[f], Nurak Grisdanurak[g]

[a]*Department of Chemical Engineering, Faculty of Engineering, KhonKaen University, KhonKaen 40002, Thailand, Tel. +668 1499 5370, email: kitirote@kku.ac.th (K. Wantala), oirnas@hotmail.com (W. Chansiriwat), k_chatkamol@kkumail.com (C. Kaewbuddee), totsaporn.s@kkumail.com (T. Suwannaruang)*
[b]*Chemical Kinetics and Applied Catalysis Laboratory (CKCL),Faculty of Engineering, KhonKaen University, KhonKaen 40002, Thailand, email: rattakh@kku.ac.th (R. Khunphonoi)*
[c]*Research Center for Environmental and Hazardous Substance Management (EHSM), Faculty of Engineering, KhonKaen University, KhonKaen 40002, Thailand*
[d]*Research Program on Development of Appropriate Technologies for Coloring Agent Removal from Textile Dyeing, Pulp & Paper, Sugar Industries for Sustainable Management, Center of Excellence on Hazardous Substance Management (HSM), Chulalongkorn University, Bangkok 10330, Thailand*
[e]*Department of Environmental Engineering, Faculty of Engineering, KhonKaen University, KhonKaen 40002, Thailand,*
[f]*Synchrotron Light Research Institute (Public Organization), Nakhon Ratchasima 30000, Thailand, email: narong@slri.or.th (N. Chanlek)*
[g]*Department of Chemical Engineering, Faculty of Engineering, Thammasat University, Pathumthani 12121, Thailand, email: gnurak@engr.tu.ac.th (N. Grisdanurak)*

Received 10 February 2019; Accepted 29 June 2019

ABSTRACT

The degradation of *para*-cresol (*p*-cresol, 100 ppm) was assisted by Cu-Fe/NaP1 catalyst heterogeneous Fenton-like process. The characterizations of Cu-Fe/NaP1 catalyst were done for surface morphology, specific surface area and oxidation state of the elements by using scanning electron microscope (SEM), N_2 adsorption-desorption apparatus and X-ray photoelectron spectroscopy (XPS), respectively. The amount of Cu-Fe mass ratio, initial pH of the solution and initial hydrogen peroxide concentration was studied as the design variable. The degradation of *p*-cresol was found that over Cu-Fe/NaP1 catalyst gave a higher performance than Cu or Fe alone. Additionally, the alloy structure between Cu and Fe was observed in $CuFeO_2$, which exhibited synergistic effects to enhance the *p*-cresol degradation efficiency. According to the design of experiment, the maximum *p*-cresol removal and initial reaction rate were computed and found at the optimum condition following, 58% Cu mass ratio, initial solution pH 4 and 120 mM of initial H_2O_2 concentration. The 4-methylcatechol, 4-hydroxybenzoic acid, 4-hydroxybenzyl alcohol and 4-hydroxybenzaldehyde intermediates were observed during the degradation reaction and demonstrated as less toxic intermediates comparing with the original substance. The degradation of *p*-cresol was achieved by the heterogeneous Fenton-like process over the Cu-Fe/NaP1 catalyst.

Keywords: Cu-Fe; NaP1; Pathway; Advanced oxidation processes; Catalytic wet peroxidation

*Corresponding author.

1. Introduction

Nowadays, the important issue regarding contaminated pollutants in surface and groundwater released from petrochemical and other industrials is still an unavoidable problem. Thus, many researchers have interested in the optimal method to degrade contaminated pollutants because of the adverse effects on human health. One of the contaminated pollutants in the effluent from petrochemical wastewater is phenolic compounds such as *p*-cresol and phenol [1]. About 30% of cresol is usually found in wastewater obtained from coal industry [2]. The *p*-cresol is isomeric substituted phenol with a methyl substitution at *para*- position [3]. Also, *p*-cresol is a highly toxic and carcinogenic substance even low concentrations [3] and is classified as group C priority pollutant by the United State Environment Protection Agency (US-EPA) because of its toxicity and persistence in the environment. Therefore, the contaminated *p*-cresol in wastewater must be treated before being released to the environment. There are many techniques applied for *p*-cresol removal such as photocatalysis [4], biological treatment process [3,5,6], adsorption [7], ozonation [8], photolysis with hydrogen peroxide [9] and Fenton process [10–12]. Fenton process is considered for organic degradation as spending the shortest reaction time approximately 2 h, compared with photocatalysis (6 h), adsorption (5 h) and biological treatment process (32 h) [3,4,7]. However, the limitation of Fenton reaction is the pH condition of reaction required to achieve at low pH at around 3.0±0.2 [11]. Moreover, the Fenton process also produces a large amount of ferric hydroxide sludge. At the end of the Fenton reaction, the iron ions leaching from the reaction is necessary to control according to the effluent standard. Many researchers have interested in preventing sludge formation by using heterogeneous catalysts through Fenton-like process, such as iron slag, Fe/supports, Cu/supports and Cu-Fe/supports [13–21], support materials including a zeolite, MCM-41 added alumina and others. Zhang and co-author used acid-activated fly ash as a Fenton-like catalyst to degrade *p*-nitrophenol [12]. Surprisingly, our previous study, we prepared NaP1 zeolite from coal fly ash power plant and it might be utilized in a heterogeneous Fenton reaction as support [22]. However, Fe/support catalysts in Fenton-like reaction give high activity only at low pH of the solution, while Cu/support catalysts can be used at higher pH of the solution [14,15,23–25]. The ozonation process, one of the advanced oxidation processes, exhibits the synergistic effect between Cu and Fe on reaction efficiency reported by many researchers [26–29]. They described that the combination of Cu and Fe shows higher oxidation reaction than Cu or Fe alone. Moreover, Cu-Fe bimetallic type can also enhance the Fenton-like reaction by preventing catalyst dissolution [30–32]. However, the influence of Cu-Fe mass ratios has been not clarified yet.

In this research, Cu-Fe bimetallic type loaded on NaP1 prepared power plant coal fly ash (Cu-Fe/NaP1) was proposed to access the effective *p*-cresol degradation through Fenton-like reaction. The physical and chemical properties of prepared Cu-Fe/NaP1 catalysts were visualized via N_2 adsorption-desorption using Brunauer–Emmett–Teller (BET) equation for calculating the specific surface area, scanning electron microscope (SEM), X-ray fluorescence (XRF) and X-ray photoelectron spectroscopy (XPS) techniques. The synergistic between Cu and Fe catalysts on *p*-cresol degradation was investigated. Moreover, main and interaction effects of independent variables such as percent weight of Cu in Cu-Fe catalysts, initial pH of the solution and initial hydrogen peroxide concentration by using Box-Behnken design were examined. The study of *p*-cresol mineralization and mechanism reaction pathway was also included.

2. Material and methods

2.1. Materials

The precursors used in this work were analytical grade and used as received without any further purification. Sodium hydroxide (NaOH), nitric acid (HNO_3), hydrochloric acid (HCl) and absolute ethanol (C_2H_5OH) were purchased from RCI Labscan Ltd., Thailand. On the other hand, hydrogen peroxide (H_2O_2), iron(III) nitrate nonahydrate ($Fe(NO_3)_3{\cdot}9H_2O$) and copper chloride ($CuCl_2$) were bought from QRëC and Ajax Finechem Pty Ltd., New Zealand. The pollutant and intermediate substances such as *p*-cresol, 4-methylcatechol, 4-hydroxybenzyl alcohol and 4-hydroxybenzaldehyde were obtained from ACROS, USA (HPLC grade). The fly ash (MFA) was collected from the Mae Moh coal power plant located in the northern part of Thailand.

2.2. Cu-Fe/NaP1 catalyst synthesis

Firstly, the synthesis steps of NaP1 supporter were followed our previous work [22]. Briefly, NaP1 was synthesized via hydrothermal method. The mole ratio of NaP1 composition was $3.0SiO_2$: $1.0Al_2O_3$: $9.2Na_2O$: $368.6H_2O$. Next, the mixed solution was transferred to a Teflon-line placed in the stainless steel autoclave and then aged in an oven at 105°C and 12 h, which is a suitable condition reported in our previous work [22]. After the hydrothermal process, the sample was separated by centrifugal technique and washed with deionized water several times until the pH of clean water lower than 9.0 then dried in an oven at 100°C. Secondly, the preparation of Cu-Fe/NaP1 was used incipient wetness impregnation technique. Ethanol volume about 6 mL same with a pore volume of NaP1 about 2 g was used as a solvent for dissolve $Fe(NO_3)_3{\cdot}9H_2O$ and $CuCl_2$ with designed amounts of Fe and Cu. After that, the mixed metal solution was slowly dropped on NaP1 with vigorous mixing about 3 min. Catalyst samples were dried at 60 and 80°C for 5 h at each temperature. Subsequently, dried catalyst samples were calcined at 500°C for 2 h in air muffle furnace.

2.3. The characterizations of catalysts

The specific surface area of the catalysts was computed from the five-point N_2-adsorption isotherms by applying the Brunauer-Emmett-Teller (BET) method. The nitrogen gas (N_2) was used to the adsorbate and operated at 77 K by using N_2 adsorption-desorption apparatus (ASAP2460, Micromeritics, USA). The surface element compositions of Cu-Fe/NaP1 were observed by X-ray photoelectron spectroscopy (XPS, ULVAC-PHI, PHI 500 VersaProbe II) using

Al Kα radiation as X-ray source at the BL5.3 SUT-NANOTEC-SLRI joint research facility, Synchrotron Light Research Institute, Thailand. The binding energy was calibrated with respect to the C 1s photoelectron line at 284.80 eV. The morphologies of Cu-Fe/NaP1 samples were investigated by using scanning electron microscope (SEM S-3000N, Hitachi, Japan). The proportional compositions of samples were analyzed by X-ray fluorescence (XRF, Bruker AXS, Germany, Model: S4 Pioneer Wavelength Dispersive X-Ray Fluorescence (WDXRF) Spectrometry) at 60 kV and 50 mA.

2.4. p-Cresol degradations

The degradation of *p*-cresol was performed over Cu-Fe/NaP1 by varying the amount of Cu-Fe loading on NaP1 and the weight ratio of Cu and Fe on NaP1. The synergistic effect of Cu and Fe on the degradation of *p*-cresol was also demonstrated. Additionally, the influences of initial pH of solution and concentrations of hydrogen peroxide were examined by using the design of experimental methodology. The Box-Behnken design was applied in this work as shown in Table 1. Finally, the mechanism pathway and kinetics of *p*-cresol degradation were studied, and demineralization of organic carbon was examined.

The initial concentration of *p*-cresol was 100 ppm, prepared by dissolved in deionized water 300 mL of reactor volume. Then, the *p*-cresol solution was adjusted pH to designed conditions by using 1.0 molar of NaOH and HCl solutions concentration. The adsorption process was done in 30 min. Next, the H_2O_2 was dropped into the *p*-cresol solution to start the degradation reaction. The remained sample was collected about 5 mL at each reaction time (0, 3, 10, 15, 30 and 60 min). After that, 2 droplets of NaOH solution were dropped into each sampling to stop the reaction, then the catalyst was filtrated by using syringe nylon membranes filter pore size 0.45 μm. The concentration of *p*-cresol was analyzed by high-performance liquid chromatography (HPLC, Waters e2695, Harlow Scientific, USA) equipped with Hypersil C18 ODS column with a UV-detector set at wavelength 250 nm. A mixture of 40% methanol (RCI Labscan Limited, HPLC grade, 99.99%) and 60% deionized water (RCI Labscan Limited, HPLC grade, 99.99%) were used as mobile phase with flow rate of 1.0 mL/min. Injection volume was 20 μL. The percent removal of *p*-cresol (at 3 min of reaction) and initial reaction rate (r_0, mM/min) were computed from Eqs. (1), (2), respectively. Both the percent removal of *p*-cresol and initial reaction rate results were used as response values, which expressed in the mathematical model calculated by using the least-square of error technique to get the coefficients of the full quadratic equation as shown in Eq. (3).

Table 1
Independent variables and levels of factors used for the optimization

Factors	Levels		
	–1	0	+1
X_1: Cu/Cu-Fe(%)	25	50	75
X_2: Initial pH of solutions	4.0	5.5	7.0
X_3: Initial hydrogen peroxide concentration (mM)	50	100	150

$$Y_1(\%) = \frac{C_0 - C_t}{C_0} \times 100 \quad (1)$$

$$Y_2 = \left(\frac{dC}{dt}\right)_0 = \frac{-3C_0 + 4C_{t1} - C_{t2}}{2\Delta t} \quad (2)$$

$$Y_{3,4}(\%) = \beta_0 + \sum_{i=1}^{3}\beta_i X_i + \sum_{i=1}^{3}\beta_i^2 X_i^2 + \sum_{i=1, j\neq i}^{3}\beta_{ij} X_i X_j + error \quad (3)$$

Here, Y_1 is experimental percent removal of *p*-cresol, and C_0 and C_t are initial and remained *p*-cresol concentration at each reaction time, respectively. Y_2 is experimental initial reaction rate and C_0 is initial *p*-cresol concentration, while C_{t1} and C_{t2} are a remained *p*-cresol concentration at the beginning of reaction, which displayed in linear trend, calculated by polynomial technique at 0.5 and 1 min, respectively. Y_3 is computed percent removal of *p*-cresol and Y_4 is computed initial reaction rate.

The concentration of intermediates were measured by gas chromatography coupled with a mass analyzer (GC-MS, GC-QP2010-MS, Shimadzu, Japan). The column was Rtx-5MS and injection volume 1 μL. The condition of GC was setup for injector at 250°C, initial oven temperature at 100°C and increasing rate about 20°C/min to final oven temperature 280°C and ion temperature of MS at 200°C. The SIM mode was used for analyst quantitative results of *p*-cresol, 4-methylcatechol, 4-hydroxybenzyl alcohol and 4-hydroxybenzaldehyde at 107, 124, 77 and 121 mz^{-1}, respectively. Total organic carbon was measured by a TOC analyzer (Multi N/C 2100s, AnalytikJena, Germany) to confirm the demineralization process.

3. Results and discussion

Firstly, the blank tests were studied following various conditions such as *p*-cresol only, *p*-cresol with NaP1 zeolite, *p*-cresol with H_2O_2 (150 mM), *p*-cresol with NaP1 zeolite and H_2O_2 (150 mM) at pH 3.0 and *p*-cresol with NaP1 zeolite and H_2O_2 (150 mM) at pH 4.0 with initial concentration of *p*-cresol 100 ppm. The results were found that *p*-cresol cannot be degraded in all conditions testing. Thus, NaP1 could not play as a catalyst, which was used as a support material in this research. Then, the degradation of *p*-cresol was primarily studied as shown in Fig. 1. The influence of the amount of Cu and Fe mass ratio was examined to exhibit the synergistic of both Cu and Fe in Fenton-like reaction. The experiment was prepared for the Fenton-like reaction by following 100 ppm of initial *p*-cresol concentration, 3.5 of initial pH of the solution, 1 g/L of catalyst loading and 150 mM of initial H_2O_2 concentration. The total content of both Fe and Cu was loaded on NaP1 at 10%wt. The results were observed that the concentration of *p*-cresol was completely removed over 100%Cu/NaP1 and 50%Cu-50%Fe/NaP1 within 3 min of the reaction, whereas the percent removal of *p*-cresol revealed only 28% degradation on 100%Fe/NaP1 in same reaction time (Fig. 1a). So that, the 100%Cu/NaP1 and 50%Cu-50%Fe/NaP1 catalysts were selected to study in the next experiment by increasing of initial pH of the solution to 4.0 and 5.0 and decreasing of catalyst loading to 0.50 g/L with 100 ppm of initial *p*-cresol concentration and 150 mM of initial H_2O_2concentration. The removal of

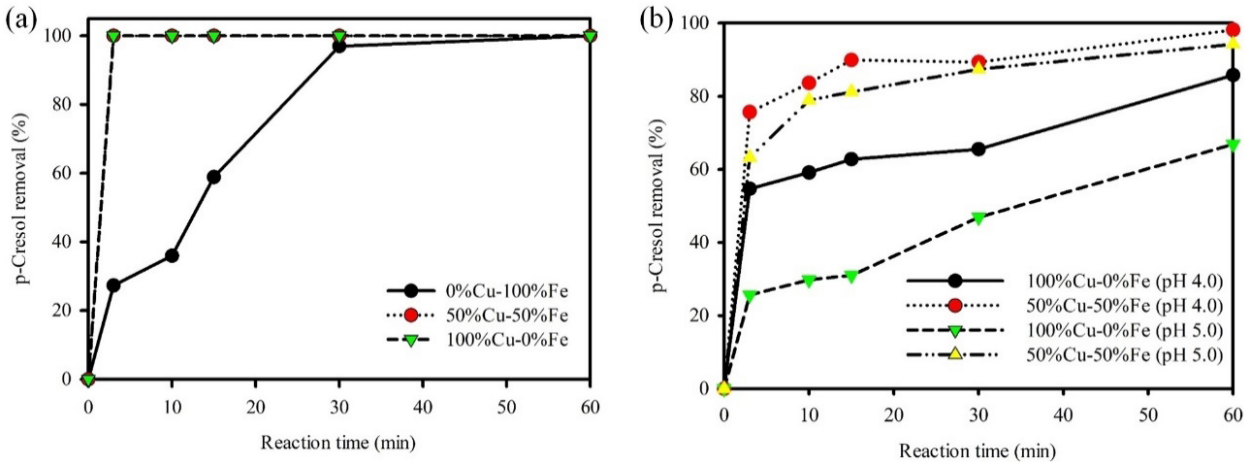

Fig. 1. *p*-Cresol degradation in effect of (a) Cu and Fe contents under 1 g/L catalyst loading and (b) initial pH of the solution under 0.10 g/L catalyst loading (100 ppm of initial *p*-cresol concentration and 150 mM of initial H_2O_2concentration).

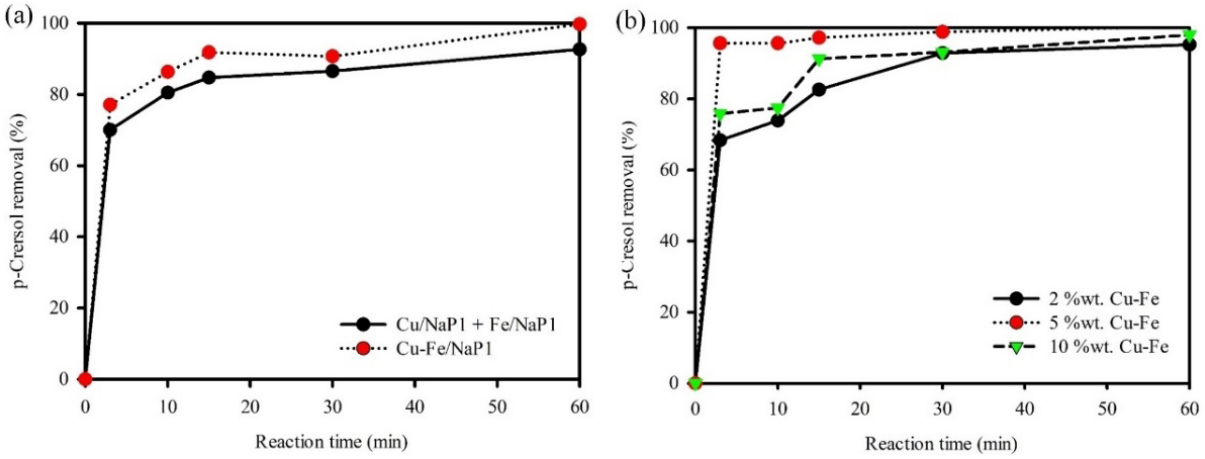

Fig. 2. *p*-Cresol degradation in (a) the synergistic effect of Cu and Fe, (b) effect of Cu-Fe loading (100 ppm of initial *p*-cresol concentration, 4 of initial pH of solution and 150 mM of initial H_2O_2 concentration).

p-cresol still showed 100% removal by 3 min of the reaction time of all initial pH of solutions. Therefore, the decrease of catalyst loading to 0.10 g/L at an initial pH of solution 4.0 and 5.0 was selected in next study. The results exhibited that 50%Cu-50%Fe/NaP1 catalyst gave higher percent removal of *p*-cresol on both initial pH values at 4.0 and 5.0 than 100%Cu/NaP1 (Fig. 1b). These results demonstrated that the composite of Cu-Fe gave the higher activity than using the only Cu in Fenton-like reaction for degradation of *p*-cresol. Additionally, the comparison of initial pH on *p*-cresol degradation by using Cu-Fe/NaP1 catalyst were investigated, as shown in the red circle and the yellow triangle line scatter. The *p*-cresol removals were slightly different. Therefore, the initial pH exhibited a little effect on *p*-cresol degradation by using Cu-Fe/NaP1 catalyst. Conversely, Cu/NaP1 catalyst with initial pH at 5.0 showed lower activity than with initial pH at 4.0 significantly. Thus, the initial pH revealed a significant effect on *p*-cresol degradation by using Cu/NaP1 catalyst.

The synergistic effect between Cu and Fe catalysts was investigated as shown in Fig. 2a by using 0.10 g/L of 10%wt. of Cu-Fe/NaP1 (50%Cu-50%Fe/NaP1) compared with mixed 100%Cu/NaP1-100%Fe/NaP1 at 100 ppm of initial *p*-cresol concentration, 4 of initial solution pH and 150 mM of initial H_2O_2 concentration. Cu and Fe contents on both catalyst types were used in the same amount to consider. The result was found that the 50%Cu-50%Fe/NaP1 catalyst showed higher removal of *p*-cresol than mixing of 100%Cu/NaP1 and 100%Fe/NaP1 catalyst. Then, the percent content of 50%Cu-50%Fe loaded on NaP1 was studied at 2%wt., 5%wt. and 10%wt. as exhibited in Fig. 2b. The experiment was done in the same amount of Cu-Fe in the reactor at about 0.01 g/L and initial *p*-cresol concentration at 100 ppm, initial pH of the solution at 4 and initial H_2O_2 concentration at 150 mM. The result was found that 5%wt. of 50%Cu-50%Fe on NaP1 displayed the highest *p*-cresol degradation. Furthermore, the specific surface area values of 2%wt., 5%wt. and 10%wt. of 50%Cu-50%Fe loaded on NaP1 were about 41, 34 and 28 m^2/g, respectively. It can be concluded that the specific surface area decreased with increasing metal contents on NaP1.

Therefore, the influence of Cu-Fe mass ratio at 5%wt. was investigated on *p*-cresol degradation, where

ratios are 25%wt. of Cu (25%Cu-75%Fe), 50%wt. of Cu (50%Cu-50%Fe)and 75%wt. of Cu (75%Cu-25%Fe), labeled as 25%Cu/Cu-Fe, 50%Cu/Cu-Fe and 75%Cu/Cu-Fe, respectively. The SEM images of various Cu contents on Cu-Fe/NaP1 are displayed in Fig. 3. The morphology of all catalysts (Fig. 3b–d) was not obviously different when compared with NaP1 (Fig. 3a). This might be due to the low contents and well dispersion of Cu-Fe on NaP1. Table 2 reveals the composition of NaP1 and Cu-Fe/NaP1 in all Cu mass ratios measured by XRF technique. The amounts of Cu compared with Fe amount without Fe content in NaP1 structure were approximately 19, 42 and 67% of designed Cu-Fe contents at 25, 50 and 75%, respectively.

The oxidation states of Cu, Fe and O atoms in Cu-Fe/NaP1 samples were analyzed by using XPS technique as displayed in Fig. 4. The spectrum intensity of both Cu $2p_{3/2}$ and Cu $2p_{1/2}$ located at 932.5 and 952 eV increased with increasing of Cu contents, whereas the Fe $2p_{3/2}$ and Fe $2p_{1/2}$ decreased. The located peaks at 932.5 and 952 eV were corresponded to Cu^{+} (Cu_2O), in addition, the peaks at 942 and 963 eV were referred to Cu^{2+} (CuO) [31,33]. Therefore, the composition of Cu-Fe/NaP1 samples was Cu_2O and CuO. Considering the peak area of Cu_2O and CuO, it was found that the amount of Cu^{+} (Cu_2O) showed higher than Cu^{2+} (CuO) (Fig. 4a). On the other hand, the binding energies of

Table 2
Composition results of NaP1 and Cu-Fe/NaP1 characterized by XRF

Compositions	NaP1	%Cu/Cu-Fe		
		25%	50%	75%
C K	7.31	11.7	0.43	– 0.31
O K	53.08	48.67	48.96	47.19
Na K	5.51	4.93	5.79	5.39
Mg K	0.87	0.75	0.86	1.01
Al K	7.14	6.25	7.99	7.63
Si K	12.24	10.58	13.35	13.15
S K	0.31	0.29	0.33	0.32
Cl K	–	0.87	2.29	3.73
K K	0.33	0.31	0.34	0.38
Ca K	8.76	6.14	8.55	9.35
Ti K	0.22	0.17	0.21	0.2
Fe K	4.22	8.37(4.15)*	8.11 (3.89)*	6.79 (2.57)*
Cu K	–	0.98	2.77	5.18
Cu(%)/Cu-Fe	–	19.10	41.59	66.84

*Fe amount without Fe content in NaP1 structure

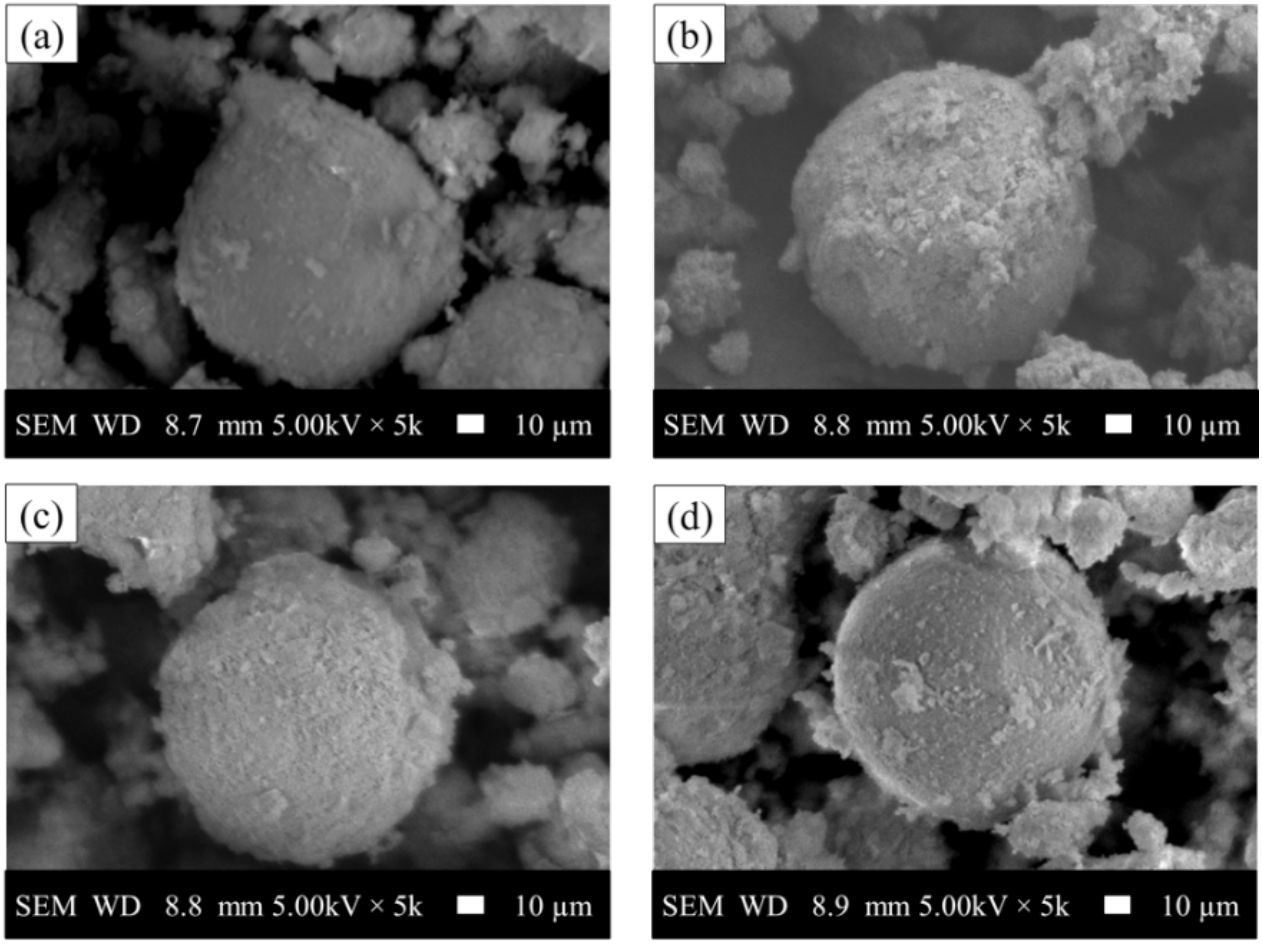

Fig. 3. SEM images of (a) NaP1 and Cu-Fe/NaP1 for (a) 25%, (c) 50%, (d) 75% of percent Cu.

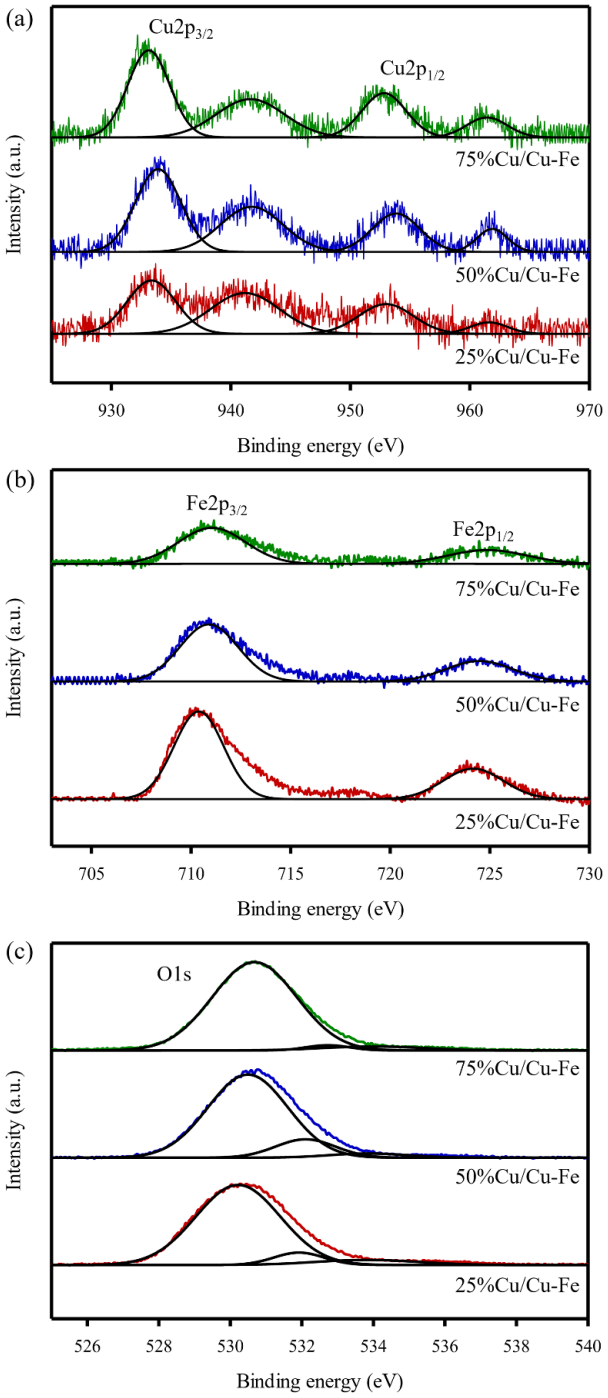

Fig. 4. The XPS results of (a) Cu 2p, (b) Fe 2p and (c) O 1s spectra of Cu-Fe/NaP1 catalysts.

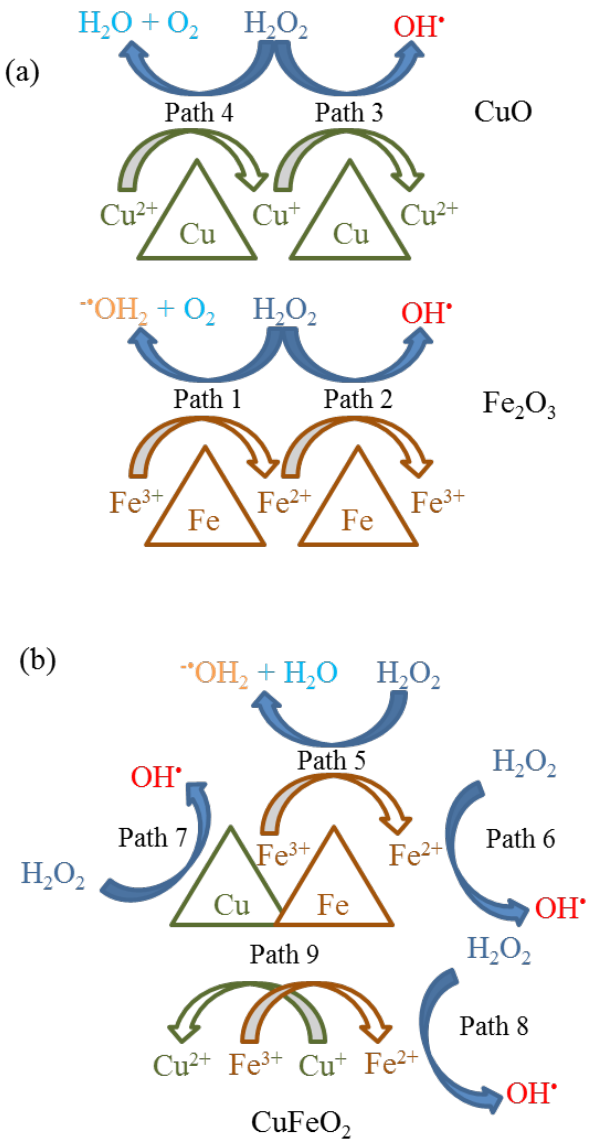

Fig. 5. Reaction mechanism of pollutant on (a) CuO and Fe_2O_3, and (b) $CuFeO_2$.

Fe were observed at 710 and 725 eV, representing to Fe^{3+}. Thus, the results can be concluded that there were the oxidation states of Cu^+, Cu^{2+} and Fe^{3+} on the surface of NaP1. Moreover, the O 1s peak was located at 530 eV, appearing in all catalysts [31]. Based on XPS results, the structures of Cu-Fe on NaP1 were mainly $CuFeO_2$ alloy phase as corresponded with the literature [31,33], besides the samples also contained CuO and Fe_2O_3 phases. The mechanisms of Fenton-like reaction were shown in Eqs. (4)–(14) and Figs. 5a and b. It can be described in 9 paths as shown in Fig. 5. Fe^{3+}–OH which is Fe^{3+} of Fe_2O_3 and $CuFeO_2$ was covered by hydroxyl radical, then reacted with H_2O_2 to form Fe^{3+}–$OH{\cdot}(H_2O_2)$ as in Eq. (4) labeled to $Fe^{3+}(H_2O_2)$, which could produce OH_2 and change to Fe^{2+} by electron exchange in Fe molecule displayed in Eq. (5) and path 1 and path 5. Then, ferrous reacted with H_2O_2 to produce continuously hydroxyl radical (Eq. (6), path 2 and path 6). Consequently, it reacted with *p*-cresol revealed in Eq. (14). Ferric was reduced to ferrous by reacted with OH_2 and O_2^- explained in Eqs. (7), (8). Moreover, Cu^+ reacted with H_2O_2 [Eq. (9), path 3 and path 7] like ferrous reaction following Haber-Weiss cycle of Fenton process. Then, producing Cu^{2+} could reduce to Cu^+ again by reacting with H_2O_2, $^{\bullet}OH_2$ and O_2^- as shown in Eqs. (10)–(13).

$$Fe^{3+}–OH + H_2O_2 \rightarrow (Fe^{3+}–OH)\cdot(H_2O_2) \quad (4)$$

$$(Fe^{3+}\cdot(H_2O_2))–OH \rightarrow Fe^{2+} + H_2O + \cdot OH_2 \quad (5)$$

$$Fe^{2+} + H_2O_2 \rightarrow Fe^{3+}–OH + \cdot OH \quad (6)$$

$$Fe^{3+}–OH + \cdot OH_2 \rightarrow Fe^{2+} + H_2O + O_2 \quad (7)$$

$$Fe^{3+}–OH + \cdot O_2^- \rightarrow Fe^{2+} + OH^- + O_2 \quad (8)$$

$$Cu^{+} + H_2O_2 \rightarrow Cu^{2+} – OH + \cdot OH \quad (9)$$

$$Cu^{2+}–OH + H_2O_2 \rightarrow (Cu^{2+}\cdot(H_2O_2)) – OH \quad (10)$$

$$(Cu^{2+}\cdot(H_2O_2)) – OH \rightarrow Cu^{+} + H_2O + O_2 \quad (11)$$

$$Cu^{2+} – OH + \cdot OH_2 \rightarrow Cu^{+} + H_2O + O_2 \quad (12)$$

$$Cu^{2+} – OH + \cdot O_2^- \rightarrow Cu^{+} + OH^- + O_2 \quad (13)$$

$$p\text{–cresol} + \cdot OH \rightarrow \ldots \rightarrow \text{degradation product} \quad (14)$$

$$Cu^{+} + Fe^{3+} \rightarrow Cu^{2+} + Fe^{2+} \quad (15)$$

The formation of Cu-Fe catalyst on NaP1 is $CuFeO_2$ alloy, the oxidation state of Cu^+ in $CuFeO_2$ structure can reduce ferric to ferrous instructures of both molecules. This can be explained by standard electrode potentials (E°) of Cu^+/Cu^{2+} and Fe^{3+}/Fe^{2+} are 0.15 V and 0.77 V, respectively. Thus, the reduction of ferric to ferrous by copper (1+) can occur as following Eq. (15) and path 9. The effective regeneration of Fe^{2+} at the surface of the catalyst can increasingly react with H_2O_2 to enhance pollutant degradation [31].

The design of the experiment was done by using Box-Behnken design (BBD) on 3 factors and 3 levels. The percent removal of *p*-cresol at 3 min of reaction time and initial reaction rate was used as responses computed by Eqs. (1) and (2), respectively. The 15 run orders were design by using MiniTab 16 and every run order was done by 3 replications. The results are shown in Table 3. The estimated regression coefficients of Eq. (3) were calculated and are shown in Table 4 for percent *p*-cresol removal and in Table 5 for the initial reaction rate.

At 95% confidence, the main parameters, including the amount of Cu, initial pH of the solution and initial H_2O_2 concentration were a significant effect on both percent *p*-cresol removal and initial reaction rate ($P_{value} < 0.05$). The square terms of all factors on percent removal of *p*-cresol were significant. On the other hand, the square terms of the amount of Cu and initial H_2O_2 concentration were significant on initial reaction rate except the square term of initial pH of the solution. However, the interaction effects of all factors were insignificant on both responses. Thus, the estimated regression coefficients were eliminated insignificant terms by using only significant terms as shown in Tables 4, 5 and Eqs. (16) and (17) for percent removal of *p*-cresol and initial reaction rate, respectively.

$$Y_3 = 94.44 + 16.70X_1 - 11.30X_2 + 10.32X_3 - 24.95X_1^2 - 3.28X_2^2 - 12.85X_3^2 \quad (16)$$

$$Y_4 = 0.37 + 0.06X_1 - 0.03X_2 + 0.04X_3 - 0.10X_1^2 - 0.05X_3^2 \quad (17)$$

Table 3
p-cresol removal and initial rate results for every standard order designed by BBD

Std Order	Cu(%)/ Cu-Fe	pH of solution	H_2O_2 (mM)	Y (%)	Initial reaction rate (mM/min)
1	25	4	100	62.46	0.25
2	75	4	100	94.57	0.33
3	25	7	100	38.80	0.20
4	75	7	100	69.03	0.29
5	25	5.5	50	30.01	0.12
6	75	5.5	50	64.24	0.25
7	25	5.5	150	47.61	0.16
8	75	5.5	150	84.70	0.37
9	50	4	50	77.43	0.31
10	50	7	50	56.95	0.23
11	50	4	150	99.78	0.40
12	50	7	150	79.10	0.31
13	50	5.5	100	95.15	0.38
14	50	5.5	100	94.09	0.37
15	50	5.5	100	94.08	0.37

Table 4
Estimated regression coefficients for Y (%)

Parameter terms	Full terms		Significant terms	
	Coefficients	P_{value}	Coefficients	P_{value}
Constant	94.44	0.000	94.44	0.000
X_1	16.70	0.000	16.70	0.000
X_2	–11.30	0.000	–11.30	0.000
X_3	10.32	0.000	10.32	0.000
X_1^2	–24.95	0.000	–24.95	0.000
X_2^2	–3.28	0.035	–3.28	0.009
X_3^2	–12.85	0.000	–12.85	0.000
X_1X_2	–0.47	0.686		
X_1X_3	0.72	0.544		
X_2X_3	–0.05	0.965		
R^2	99.65		99.61	
R^2_{adj}	99.02		99.31	

Here, Y_3 and Y_4 are calculated responses of percent removal of *p*-cresol and initial reaction rate, respectively. X_1, X_2 and X_3 are coded independent variables.

The error of experiment orders was checked by using the normal probability of standard error for both responses as displayed in Fig. 6. The equations of full quadratic terms and significant terms of both responses were compared with experimental results. According to $P_{value} > 0.05$ of both responses, the significant errors were not found in every running order. Additionally, the comparison of the experimental results with the predicted results exhibited that every run order was closed to each other for *p*-cresol

Table 5
Estimated regression coefficients for initial reaction rate

Parameter terms	Full terms		Significant terms	
	Coefficients	P_{value}	Coefficients	P_{value}
Constant	0.37	0.000	0.37	0.000
X_1	0.06	0.002	0.06	0.000
X_2	−0.03	0.028	−0.03	0.007
X_3	0.04	0.011	0.04	0.002
X_1^2	−0.10	0.002	−0.10	0.000
X_2^2	−0.01	0.582		
X_3^2	−0.05	0.021	−0.05	0.005
X_1X_2	0.00	0.874		
X_1X_3	0.02	0.240		
X_2X_3	−0.00	0.874		
R^2	95.62		93.71	
R^2_{adj}	87.73		90.21	

removal (Fig. 7a) and initial reaction rate (Fig. 7b). R^2 and R^2_{adj} of percent removal of *p*-cresol for the full quadratic term were about 99.65 and 99.02%, respectively. A small different value between R^2 and R^2_{adj} suggested that the insignificant terms can be negligible or removed from the full quadratic equation. Then, R^2 and R^2_{adj} of the percentage of *p*-cresol removal for the significant terms were approximately 99.61 and 99.31%, respectively. Furthermore, R^2 and R^2_{adj} of initial reaction rate for the full quadratic terms were about 95.62 and 87.73%, respectively. However, R^2 and R^2_{adj} of initial reaction rate for the significant terms were about 93.71 and 90.21%, respectively, approaching 100%. Thus, the predicted significant equations can explain the main effect, interaction effect and optimal condition of both responses.

The ANOVA results were used to confirm the precision of the predicted equation by using 95% confidence (Table 6). Regarding the response of percent removal of *p*-cresol, the regression term was significant ($P_{value} < 0.05$) because F_{value} (337.75) showed higher than $F_{critical}$ ($F_{(0.05,6,8)} = 3.58$). The main effect and square terms were significant proven by F_{value} which was higher than $F_{critical}$ ($F_{(0.05,3,8)} = 4.07$). Comparing each variable, Cu content showed higher affectable than

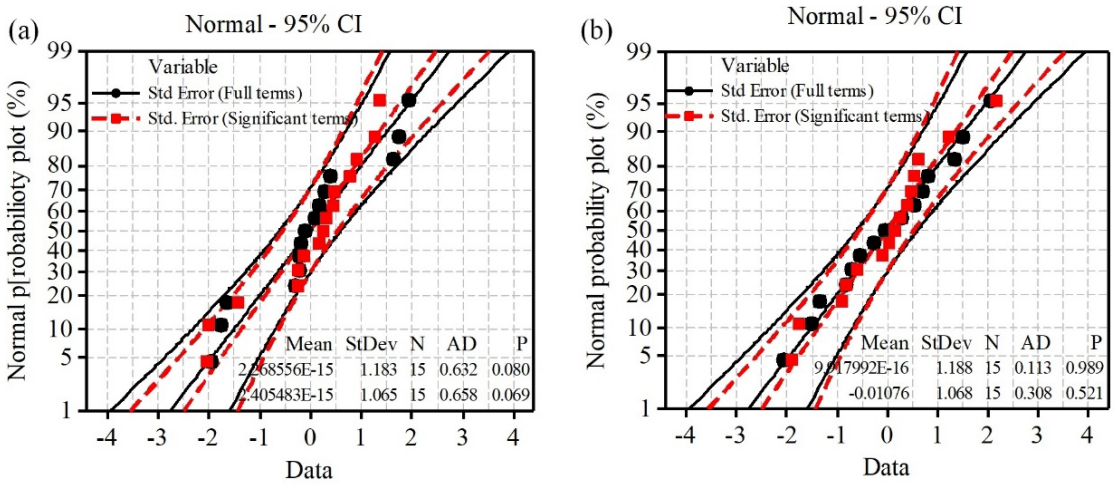

Fig. 6. Normal probability of standard error compared between experimental results and computed results of (a) percent removal of *p*-cresol and (b) initial reaction rate.

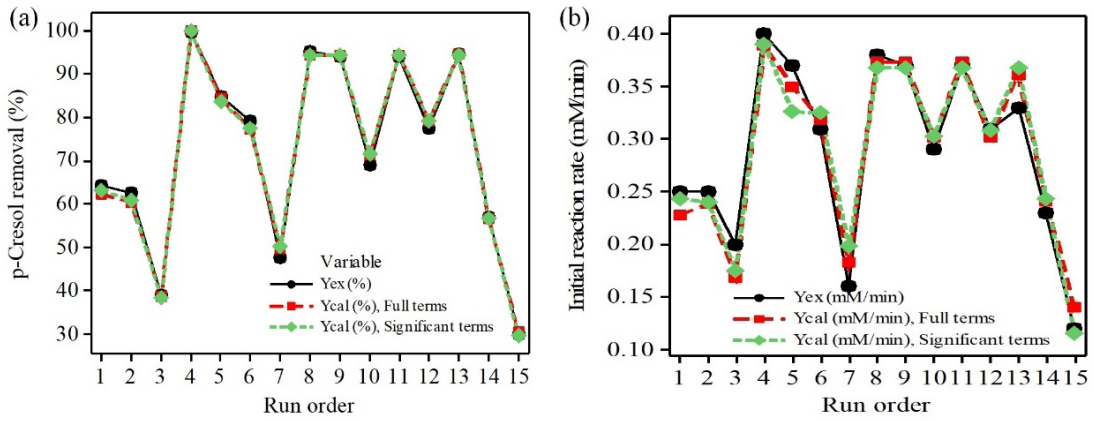

Fig. 7. Time series of experimental results and computed results of (a) percent removal of *p*-cresol and (b) initial reaction rate.

Table 6
ANOVA for percent removal of *p*-cresol and initial reaction rate of significant terms

Percent removal of *p*-cresol at 3 min of reaction time				
Sources	DF	F_{value}	P_{value}	Results
Regression	6	337.75	0.000	Significant
Linear	3	404.92	0.000	Significant
X_1	1	660.71	0.000	Significant
X_2	1	301.97	0.000	Significant
X_3	1	252.08	0.000	Significant
Square	3	270.57	0.000	Significant
X_1^2	1	680.04	0.000	Significant
X_2^2	1	11.72	0.009	Significant
X_3^2	1	180.39	0.000	Significant
Residual Error	8			
Lack-of-Fit	6	11.59	0.082	Insignificant
Pure Error	2			
Total	14			
Initial reaction rate				
Sources	DF	F_{value}	P_{value}	Results
Regression	5	26.79	0.000	Significant
Linear	3	25.38	0.000	Significant
X_1	1	45.35	0.000	Significant
X_2	1	11.79	0.007	Significant
X_3	1	18.99	0.002	Significant
Square	2	28.92	0.000	Significant
	1	47.71	0.000	Significant
	1	13.46	0.005	Significant
Residual error	9			
Lack-of-fit	7	27.37	0.036	Significant
Pure error	2			
Total	14			

other effects, initial pH of the solution and initial H_2O_2 concentration, according to F_{value} about 660.71, 301.97 and 252.57, respectively. Comparing square term of each variable, Cu content still showed the highest effect whereas initial H_2O_2 concentration showed a higher effect than initial pH of solution referring to F_{value} about 680.04, 180.39 and 11.72, respectively. On the other hand, for the response of initial reaction rate, the regression term was significant ($P_{value} < 0.05$) because F_{value} (26.79) was higher than $F_{critical}$ ($F_{(0.05,5,9)} = 3.48$). The main and square terms was significantly confirmed by F_{value} about 25.38 and 28.92 and showed higher than $F_{critical}$ ($F_{(0.05,3,9)} = 3.86$ and $F_{(0.05,2,9)} = 4.26$). Considering the variable effect, it can be noted that Cu content showed the highest effect, following by initial H_2O_2 concentration and initial pH of the solution with F_{value} about 45.35, 18.99 and 11.79, respectively. Additionally, the square term of the influence of Cu content also showed higher than initial H_2O_2 concentration, while the initial pH of the solution was an insignificant effect on this response. Lack of Fit (LOF) term was considered for both percent removal of *p*-cresol and initial reaction rate responses. F_{values} of LOF term were 11.59 and 27.37 for percent degradation of *p*-cresol and initial reaction rate responses, respectively. The F_{value}(LOF) of percent degradation of *p*-cresol response was lower than $F_{critical}$ ($F_{(0.05,6,2)} = 19.33$) and higher than P_{value} significant value (0.05) about 0.082, which can be described that the Lack of Fit of predicted results was insignificant. On the other hand, the F_{value}(LOF) of initial reaction rate response was slightly higher than $F_{critical}$ ($F_{(0.05,6,2)} = 19.33$) and lower than P_{value} significant value (0.05) about 0.036, which can be described that the Lack of Fit of predicted results was significant. However, R^2 and R^2_{adj} closed to 100% in which the predicted equation have a good approximation for the experimental values [34]. Therefore, showing of high value for R^2 correlation between predicted results and experiment results of both equations could be used to compute the influence of Cu content, initial pH of the solution and initial H_2O_2 concentration on the percentage of *p*-cresol removal and initial reaction rate.

Although the interaction effects of parameter variables were statistically insignificant on both responses, the contour plots were clearly found the interaction between Cu content and initial H_2O_2 concentration as shown in Fig. 8. According to Figs. 8a, b, d and e, the results demonstrated that the percent decomposition of *p*-cresol and initial reaction rate increased with increasing Cu ratio of Cu-Fe on NaP1. The more Cu contents in Cu-Fe enhanced the performance of Fenton reaction due to increasing the amounts Cu^{1+} to react with H_2O_2. As a results, OH radical increasingly generated and continuously reacted with pollutants according to Eqs. (9) and (14). However, both responses decreased when the mass ratio of Cu exceeded 70%. The excessive Cu^{1+} on $CuFeO_2$ reacted with OH radical, in which the performance of catalysts decreased as displayed in Eq. (18).

$$Cu^{1+} + OH^{\cdot} \rightarrow Cu^{2+} + OH^{-} \quad (18)$$

$$H_2O_2 + OH^{\cdot} \rightarrow H_2O + HOO^{\cdot} \quad (19)$$

$$HOO^{\cdot} + OH^{\cdot} \rightarrow H_2O + O_2 \quad (20)$$

Figs. 8a, c, d and f reveal that the percent removal *p*-cresol and initial reaction rate decreased with increasing of initial pH of solutions from 4.0 to 7.0. This because hydrogen peroxide could degrade to water at high pH condition resulting in OH radicals formed in low amounts [31,35]. Considering the influence of initial H_2O_2 concentration effect (Figs. 8b, c, e and f), the percent removal *p*-cresol and initial reaction rate increased with increasing the initial concentration of H_2O_2. This described that the increase of initial H_2O_2 concentration gave higher production of OH radicals as following Haber-Weiss mechanism (Eqs. (6), (9) and (14)). However, the reactivity of catalyst inhibited when the concentration of initial H_2O_2 concentration exceeded 125 ppm. The high amount of H_2O_2 concentration could react with OH· to form water and ·OOH, subsequently reacted with OH· for the formation of water and oxygen as displayed in Eqs. (19) and (20), respectively [30,36]. The optimal conditions of both responses were calculated by Eqs. (16) and (17). The maximal condition of percent removal of *p*-cresol and initial reaction rate showed the same values, which was Cu about 58%, initial pH of solution about 4.0 and initial H_2O_2 concentration about 120 mM, resulting in 107% for *p*-cresol removal and 0.419 mM/min

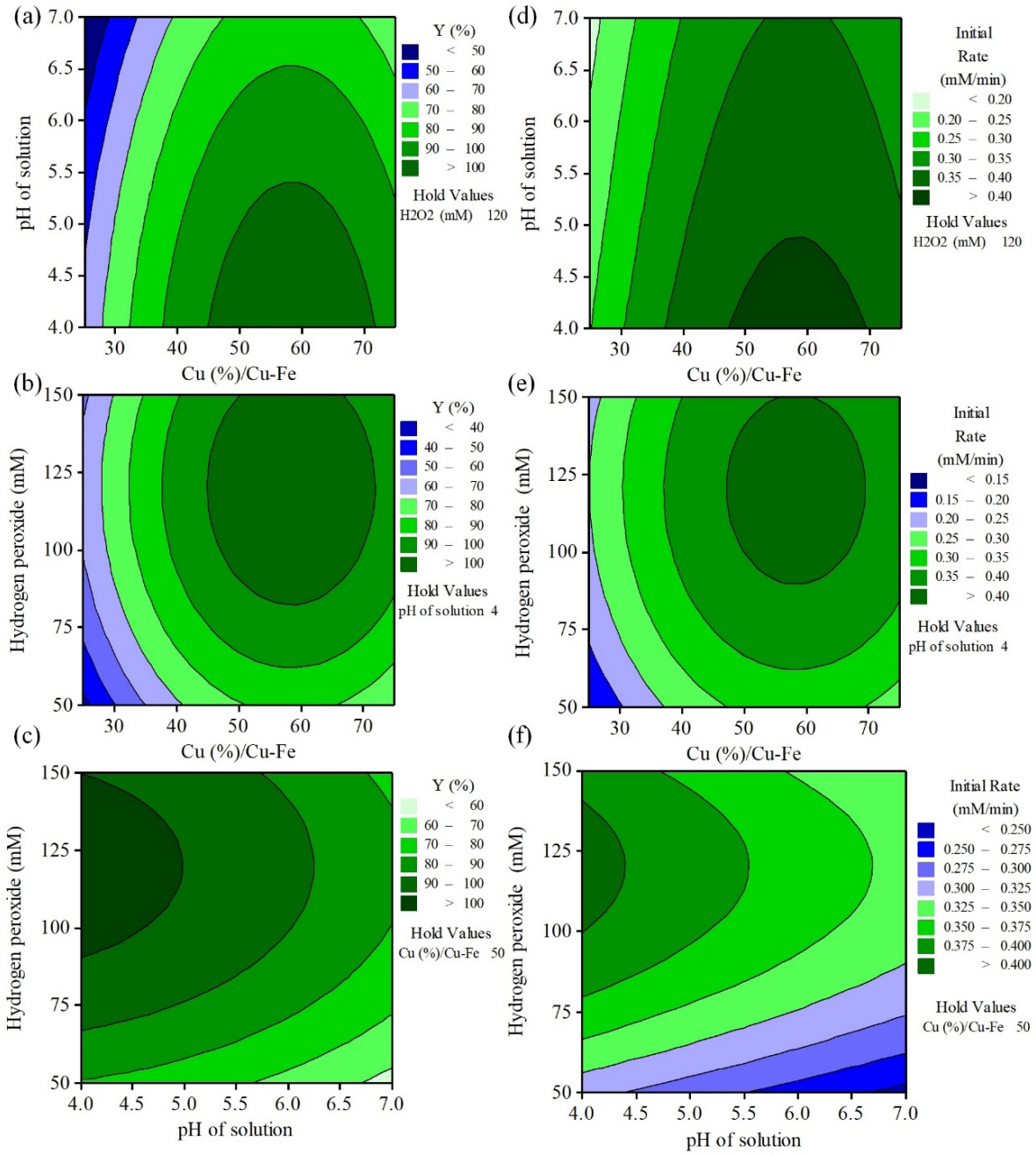

Fig. 8. Contour plots of interaction effects: (a, b, c) percent removal of *p*-cresol and (d, e, f) initial reaction rate.

for the initial reaction rate. Therefore, predicted equations were verified by using 50% of Cu, 5.5 of initial pH of the solution and 120 mM of initial H_2O_2 concentration for triplicate runs. The computed results were approximately 96.51% and 0.376 mM/min whereas the experimental results were 87.34±2.42% and 0.344±0.0095 mM/min of percent degradation of *p*-cresol and initial reaction rate, respectively. The experimental results showed slightly lower than predicted results of both terms. It could be described by F_{value} and P_{value} of LOF. P_{value} were approximately 0.082 and 0.036 of percent removal of *p*-cresol and initial reaction rate. Besides, P_{value} showed a little lower than the insignificant error of precision ($P_{value} > 0.05$). However, these results were different approximately lower than 10%. The leach of Cu and Fe was investigated by collecting the sample carried out for 120 min and measured by using atomic absorption spectrometer (AAS, Perkin Elmer AAnalyst 300, USA). The concentrations of leaching Cu and Fe were found at 0.047 and 0.008 ppm, respectively. This can be noted that the Fenton reaction takes place on the heterogeneous reaction called Fenton-like reaction. Additionally, the concentrations of leaching metals were lower than standards for effluent discharge regulations of factory wastewater announced from Ministry of industry, Thailand [37].

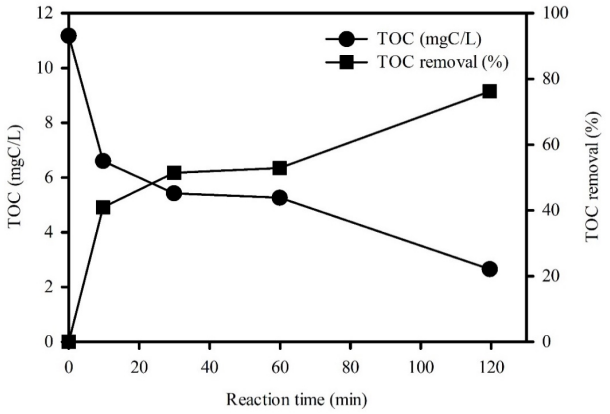

Fig. 9. Total organic carbon of the samples vs. reaction times.

Furthermore, total organic carbon (TOC) was studied, indicating the degree of mineralization of Fenton-like reaction as shown in Fig. 9. It was found that the TOC profile was sharply decreased at the first 20 min of reaction time then slightly decreased until 120 min of reaction time. At final reaction time, TOC can be removed approximately 8.52 mg C/L or 76% of TOC removal. Since *p*-cresol was degraded to various intermediate via Fenton-like reaction, the intermediate formation was investigated by using gas chromatography-mass spectroscopy (GC-MS). The intermediates of 4-methylcatechol, 4-hydroxybenzyl alcohol, 4-hydroxybenzaldehyde and 4-hydroxybenzoic acid were found in the solutions. The intermediate chemicals were found similar to other researchers, who studied the oxidation reaction of *p*-cresol by ozonation [8] and photocatalytic reaction [38–40]. Thus, the mechanism of *p*-cresol degradation can be purposed as displayed in Fig. 10.

The intermediates, 4-methylcatechol (B), 4-hydroxybenzyl alcohol (C), 4-hydroxybenzaldehyde (D) and 4-hydroxybenzoic acid (E), were found at 3 min of reaction time. After 1 h of reaction time, the intermediates were disappeared because they were degraded to aromatic opened ring products and accordingly degraded to CO_2 and water [9,40]. However, 4-hydroxybenzoic acid was found in very low signal which could not measure in quantitative concentration. According to the mechanism pathways of *p*-cresol degradation, OH· could possibly react on two positions, including ortho- and methyl group- positions of *p*-cresol. If OH radicals attach at the ortho- position, 4-methylcatechol would be produced. On the contrary, if OH radicals attach on the methyl group-position, 4-hydroxybenzyl alcohol, 4-hydroxybenzaldehyde and 4-hydroxybenzoic acid would be generated [8,40]. The kinetic reaction can be purposed by elementary rate laws as shown in Eqs. (21)–(23). The concentrations of *p*-cresol, 4-methylcatechol and 4-hydroxybenzyl alcohol were labeled C_A, C_B and C_C, respectively. The concentrations of all chemicals were used from GC-MS results at 0, 3 and 10 min of reaction times. The Gauss-Jordan technique was used to calculate the reaction rate constants. The calculated results were displayed in Eqs. (24)–(26). The reaction rate constants were 4.69, 22.41, 0.34, and 1.56 min^{-1} for k_1, k_2, k_3 and k_4, respectively. According to reaction rate constant values, it can be explained that *p*-cresol preferred

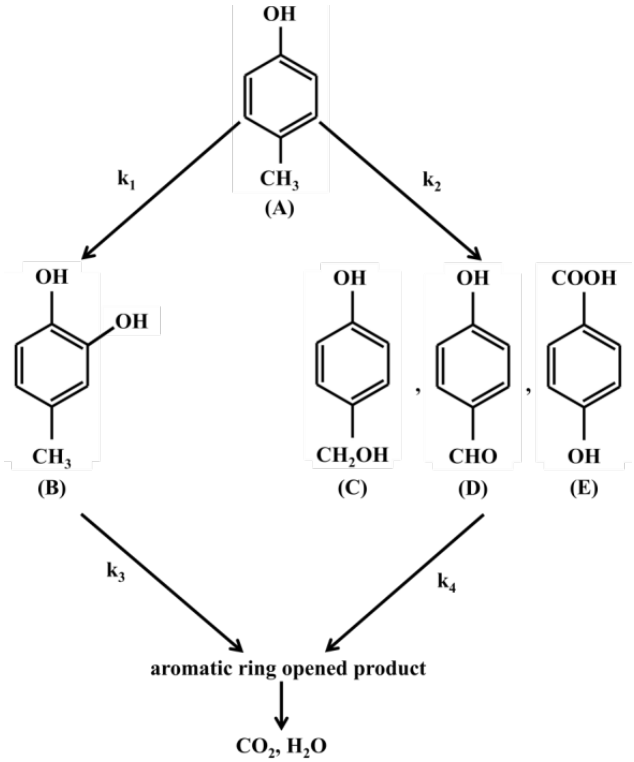

Fig. 10. Mechanism pathway for *p*-cresol degradations.

to be reacted at methyl group- position more than ortho-position to form 4-methylcatechol.

$$dC_A/dt = -(k_1 + k_2)C_A \quad (21)$$

$$dC_B/dt = k_1C_A - k_3C_B \quad (22)$$

$$dC_C/dt = k_2C_A - k_4C_c \quad (23)$$

$$dC_A/dt = -27.10C_A \quad (24)$$

$$dC_B/dt = 4.69C_A - 0.34C_B \quad (25)$$

$$dC_C/dt = 22.41C_A - 1.56C_c \quad (26)$$

The *p*-cresol was almost completely degraded at reaction time lower than 10 min then changed to the formation of intermediates. The intermediates were therefore decomposed to CO_2 and H_2O confirmed by the TOC results. Table 7 shows the hazard identification of pollutant and intermediates. *p*-cresol is acute toxicity dermal and oral (Cat. 3) and skin corrosion (Cat. 1B) classified to danger category, while all of the intermediates are classified to warning category or less toxicity than an initial pollutant. Although, 4-hydroxybenzyl alcohol cannot even be completely demineralized until 120 min to carbon dioxide and water, this chemical was classified to warning category.

Table 7
The hazard identification of reactant and intermediate chemicals

Chemicals	Hazard identification according to Regulation (EC) No 1272/2008	
	Category	Symbol
p-cresol	Acute toxicity Dermal (Cat. 3) Acute toxicity Oral (Cat. 3) Skin corrosion (Cat. 1B)	 Danger[a]
4-methylcatechol	Skin irritation (Cat. 2) Eye irritation (Cat. 2) Specific target organ toxicity single exposure (Cat. 3) (respiratory irritation)	 Warning[b]
4-hydroxybenzyl alcohol	Skin irritation (Cat. 2) Eye irritation (Cat. 2) Specific target organ toxicity single exposure (Cat. 3) (respiratory irritation)	 Warning[b]
4-hydroxybenzaldehyde	Eye irritation (Cat. 2)	 Warning[b]
4-hydroxybenzoic acid	Skin irritation (Cat. 2) Eye irritation (Cat. 2) Specific target organ toxicity single exposure (Cat. 3) (respiratory irritation)	 Warning[b]

[a]Danger means a signal word indicating the more severe hazard categories.
[b]Warning means a signal word indicating the less severe hazard categories.

4. Conclusions

Cu-Fe on NaP1 support was synthesized to $CuFeO_2$ alloy referring to the oxidation state of Cu and Fe elements. The synergistic effect between Cu and Fe in $CuFeO_2$ alloy was observed to be an effect on *p*-cresol degradation. The Fenton-like reaction over Cu-Fe/NaP1 can be achieved at neutral pH of the solution. *p*-cresol was completely degraded at the reaction time less than 10 min. In the Fenton-like reaction of *p*-cresol degradation, 4-methylcatechol, 4-hydroxybenzyl alcohol, 4-hydroxybenzaldehyde and 4-hydroxybenzoic acid were generated. However, all intermediates presented less toxicity, compared with the original substance. The degradation pathway of *p*-cresol exhibited that OH radicals preferred to react with *p*-cresol at the position of the methyl group to form 4-methylcatechol. The mineralization of pollutants showed about 76 percent removal for 2 h of reaction time.

Acknowledgments

Authors would like to acknowledge the financial support from the Research Center for Environmental and Hazardous Substance Management (EHSM), KhonKaen University and the Office of Higher Education Commission (OHEC) and the S&T Postgraduate Education and Research Development Office (PERDO) through Research Program on Development of Appropriate Technologies for Coloring Agent Removal from Textile Dyeing, Pulp & Paper, Sugar Industries for Sustainable Management, Center of Excellence on Hazardous Substance Management (HSM), Chulalongkorn University, Bangkok, Thailand. The authors would also like to express their gratitude to Synchrotron Light Research Institute (Public Organization), Thailand for XPS measurement (SUT-NANOTEC-SLRI: BL. 5.3) and the Center of Excellence on Hazardous Substance Management (HSM) Chulalongkorn University and the Advanced Functional nanomaterials & Membrane for Environmental Remediation (AFMER) Research Unit for their invaluable support in terms of facilities and scientific equipment.

References

[1] S. Esplugas, J. Giménez, S. Contreras, E. Pascual, M. Rodríguez, Comparison of different advanced oxidation processes for phenol degradation, Water Res., 36 (2002) 1034–1042.
[2] G.S. Veeresh, P. Kumar, I. Mehrotra, Treatment of phenol and cresols in upflow anaerobic sludge blanket (UASB) process: a review, Water Res., 39 (2005) 154–170.
[3] A. Hamitouche, Z. Bendjama, A. Amrane, F. Kaouah, D. Hamane, R. Ikkene, Biodegradation of P-cresol by mixed culture in batch reactor – effect of the three nitrogen sources used, Procedia. Eng., 33 (2012) 458–464.

[4] C.M. Gómez, G. Del Angel, F. Tzompantzi, R. Gómez, L.M. Torres-Martínez, Photocatalytic degradation of p-cresol on Pt/γAl_2O_3–TiO_2 mixed oxides: Effect of oxidizing and reducing pre-treatments, J. Photochem. Photobiol. A Chem., 236 (2012) 21–25.
[5] S. Kumar, D. Arya, A. Malhotra, S. Kumar, B. Kumar, Biodegradation of dual phenolic substrates in simulated wastewater by Gliomastix indicus MTCC 3869, J. Environ. Chem. Eng., 1 (2013) 865–874.
[6] E. Xenofontos, A.-M. Tanase, I. Stoica, I. Vyrides, Newly isolated alkalophilic Advenella species bioaugmented in activated sludge for high p-cresol removal, N. Biotechnol., 33 (2016) 305–310.
[7] J. Huang, Treatment of phenol and p-cresol in aqueous solution by adsorption using a carbonylated hypercrosslinked polymeric adsorbent, J. Hazard. Mater., 168 (2009) 1028–1034.
[8] S.H. Kow, M.R. Fahmi, C. Zulzikrami, A. Abidin, S.-A. Ong, Oxidation of p-cresol by ozonation, Sains Malaysiana., 47 (2018) 1085–1091.
[9] T. Zhang, L. Cheng, L. Ma, F. Meng, R.G. Arnold, A.E. Sáez, Modeling the oxidation of phenolic compounds by hydrogen peroxide photolysis, Chemosphere, 161 (2016) 349–357.
[10] S. Karthikeyan, V.K. Gupta, R. Boopathy, A. Titus, G. Sekaran, A new approach for the degradation of high concentration of aromatic amine by heterocatalytic Fenton oxidation: Kinetic and spectroscopic studies, J. Mol. Liq., 173 (2012) 153–163.
[11] V. Kavitha, K. Palanivelu, Destruction of cresols by Fenton oxidation process, Water Res., 39 (2005) 3062–3072.
[12] A. Zhang, N. Wang, J. Zhou, P. Jiang, G. Liu, Heterogeneous Fenton-like catalytic removal of p-nitrophenol in water using acid-activated fly ash, J. Hazard. Mater., 201–202 (2012) 68–73.
[13] M.E.M. Ali, T.A. Gad-Allah, M.I. Badawy, Heterogeneous fenton process using steel industry wastes for methyl orange degradation, Appl. Water Sci., 3 (2013) 263–270.
[14] P. Bautista, A.F. Mohedano, J.A. Casas, J.A. Zazo, J.J. Rodriguez, Highly stable Fe/γ-Al_2O_3 catalyst for catalytic wet peroxide oxidation, J. Chem. Technol. Biotechnol., 86 (2011) 497–504.
[15] J.G. Carriazo, E. Guelou, J. Barrault, J.M. Tatibouët, S. Moreno, Catalytic wet peroxide oxidation of phenol over Al–Cu or Al–Fe modified clays, Appl. Clay Sci., 22 (2003) 303–308.
[16] A. Rey, M. Faraldos, J.A. Casas, J.A. Zazo, A. Bahamonde, J.J. Rodríguez, Catalytic wet peroxide oxidation of phenol over Fe/AC catalysts: Influence of iron precursor and activated carbon surface, Appl. Catal. B Environ., 86 (2009) 69–77.
[17] A. Rey, A.B. Hungria, C.J. Duran-Valle, M. Faraldos, A. Bahamonde, J.A. Casas, J.J. Rodriguez, On the optimization of activated carbon-supported iron catalysts in catalytic wet peroxide oxidation process, Appl. Catal. B Environ., 181 (2016) 249–259.
[18] Y. Wang, H. Zhao, M. Li, J. Fan, G. Zhao, Magnetic ordered mesoporous copper ferrite as a heterogeneous Fenton catalyst for the degradation of imidacloprid, Appl. Catal. B Environ., 147 (2014) 534–545.
[19] Q. Wu, X. Hu, P.L. Yue, X.S. Zhao, G.Q. Lu, Copper/MCM-41 as catalyst for the wet oxidation of phenol, Appl. Catal. B Environ., 32 (2001) 151–156.
[20] Y. Yan, S. Jiang, H. Zhang, Efficient catalytic wet peroxide oxidation of phenol over Fe-ZSM-5 catalyst in a fixed bed reactor, Sep. Purif. Technol., 133 (2014) 365–374.
[21] L. Zhang, Y. Nie, C. Hu, J. Qu, Enhanced Fenton degradation of Rhodamine B over nanoscaled Cu-doped $LaTiO_3$ perovskite, Appl. Catal. B Environ., 125 (2012) 418–424.
[22] W. Chansiriwat, D. Tanangteerapong, K. Wantala, Synthesis of zeolite from coal fly ash by hydrothermal method without adding alumina and silica sources: Effect of aging temperature and time, Sains Malaysiana., 45 (2016).
[23] K. Wantala, C. Khamjumphol, N. Thananukool, A. Neramittagapong, Degradation of Reactive Red 3 by heterogeneous Fenton-like process over iron-containing RH-MCM-41 assisted by UV irradiation, Desal. Water Treat., 54 (2015) 699–706.
[24] R.M. Liou, S.-H. Chen, CuO impregnated activated carbon for catalytic wet peroxide oxidation of phenol, J. Hazard. Mater., 172 (2009) 498–506.
[25] C. di Luca, P. Massa, R. Fenoglio, F.M. Cabello, Improved Fe_2O_3/Al_2O_3 as heterogeneous Fenton catalysts for the oxidation of phenol solutions in a continuous reactor, J. Chem. Technol. Biotechnol., 89 (2014) 1121–1128.
[26] H. He, Y. Liu, D. Wu, X. Guan, Y. Zhang, Ozonation of dimethyl phthalate catalyzed by highly active CuxO-Fe_3O_4 nanoparticles prepared with zero-valent iron as the innovative precursor, Environ. Pollut., 227 (2017) 73–82.
[27] F. Qi, W. Chu, B. Xu, Comparison of phenacetin degradation in aqueous solutions by catalytic ozonation with $CuFe_2O_4$ and its precursor: Surface properties, intermediates and reaction mechanisms, Chem. Eng. J., 284 (2016) 28–36.
[28] F. Qi, W. Chu, B. Xu, Ozonation of phenacetin in associated with a magnetic catalyst $CuFe_2O_4$: The reaction and transformation, Chem. Eng. J., 262 (2015) 552–562.
[29] X. Liu, Z. Zhou, G. Jing, J. Fang, Catalytic ozonation of Acid Red B in aqueous solution over a Fe–Cu–O catalyst, Sep. Purif. Technol., 115 (2013) 129–135.
[30] M. Xia, M. Long, Y. Yang, C. Chen, W. Cai, B. Zhou, A highly active bimetallic oxides catalyst supported on Al-containing MCM-41 for Fenton oxidation of phenol solution, Appl. Catal. B Environ., 110 (2011) 118–125.
[31] X. Zhang, Y. Ding, H. Tang, X. Han, L. Zhu, N. Wang, Degradation of bisphenol A by hydrogen peroxide activated with $CuFeO_2$ microparticles as a heterogeneous Fenton-like catalyst: Efficiency, stability and mechanism, Chem. Eng. J., 236 (2014) 251–262.
[32] Y. Ding, L. Zhu, N. Wang, H. Tang, Sulfate radicals induced degradation of tetrabromobisphenol A with nanoscaled magnetic $CuFe_2O_4$ as a heterogeneous catalyst of peroxymonosulfate, Appl. Catal. B Environ., 129 (2013) 153–162.
[33] S.P. Pavunny, A. Kumar, R.S. Katiyar, Raman spectroscopy and field emission characterization of delafossite $CuFeO_2$, J. Appl. Phys., 107 (2010) 013522.
[34] M.D. De luna, L.J.M. Millanar, A. Yodsa-Nga, K. Wantala, Gas phase catalytic oxidation of VOCS using hydrothermally synthesized nest-like K-OMS 2 catalyst, Sains Malaysiana., 46 (2017) 275–283.
[35] S. Zha, Y. Cheng, Y. Gao, Z. Chen, M. Megharaj, R. Naidu, Nanoscale zero-valent iron as a catalyst for heterogeneous Fenton oxidation of amoxicillin, Chem. Eng. J., 255 (2014) 141–148.
[36] R. Idel-aouad, M. Valiente, A. Yaacoubi, B. Tanouti, M. López-Mesas, Rapid decolourization and mineralization of the azo dye C.I. Acid Red 14 by heterogeneous Fenton reaction, J. Hazard. Mater., 186 (2011) 745–750.
[37] M. of Industry, Standards for effluent of factory wastewater, Ministry of Industry annoucement, 2018. http://www.diw.go.th/hawk/news/11.PDF (accessed September 26, 2018).
[38] Y. Abdollahi, A.H. Abdullah, Z. Zainal, N.A. Yusof, Photocatalytic degradation of p-cresol by zinc oxide under UV irradiation, Int. J. Mol. Sci., 13 (2012) 302–315.
[39] R. Khunphonoi, N. Grisdanurak, Mechanism pathway and kinetics of p-cresol photocatalytic degradation over titania nanorods under UV–visible irradiation, Chem. Eng. J., 296 (2016) 420–427.
[40] A. Han, J. Sun, X. Lin, C.-H. Yuan, G.K. Chuah, S. Jaenicke, Influence of facets and heterojunctions in photoactive bismuth oxyiodide, RSC Adv., 5 (2015) 88298–88305.